Title: Atomic Ejecta Source Optical Probe (AESOP) FY2021 Work Package L3 Milestone Report

Author(s): Schauer, Martin Michael
Paisner, Jeffrey Alan
Stevens, G. D.

Intended for: Report

Issued: 2021-08-18

Atomic Ejecta Source Optical Probe (AESOP)

FY2021 Work Package L3 Milestone Report

M. M. Schauer[1], J.A. Paisner,[1] and G.D. Stevens[2]

[1]Los Alamos National Laboratory, Los Alamos, NM
[2]Nevada National Security Site, Special Technologies Laboratory, Santa Barbara, CA

August 10, 2021

1 Introduction

As part of its mission to ensure the reliability of the nation's nuclear weapons stockpile, the NNSA has funded a broad range of projects to characterize the mass of material ejected from shocked metal surfaces with special emphasis placed on determining the size distribution of macroscopic "ejecta" particles. Substantial work has been done for particles with diameters down to roughly 1 μm, but little data is available for smaller particles, and no data exist for the amount of atomic-scale ejecta produced in such dynamic environments. Such data are important due to the implications for weapons systems behavior but also for distinguishing between different potential ejecta production mechanisms, such as Rayleight-Taylor instability or the shallow-bubble-collapse phenomenon recently proposed by G. Maskally.

Here we report on progress in developing a diagnostic capable of measuring the atomic vapor column densities evolved from shocked metal surfaces in real time at probed-level column densities on the order of tens of ng/cm^2 or lower. The technique relies on the dispersion produced by an electronic transition in an atomic vapor[1]. Briefly, the different frequency sidebands present in a sinusoidally phase-modulated laser beam tuned near an electronic resonance of the atomic vapor under study will experience differing degrees of dispersion and absorption as the beam traverses the vapor. The various sidebands will then combine on the face of any detector with sufficient bandwidth to produce interference. In short, they beat against each other.

The technique, though conceptually simple, requires high quality, spectroscopic data for the element of interest; highly engineered lasers and electro-optical devices; high speed, low noise detectors; and high speed data acquisition systems. Thanks to rapidly developing diode laser technology and high speed electronics, the hardware necessary for a robust, fieldable diagnostic is now available, and decades of careful experimentation have provided the atomic spectroscopy data needed to make such a diagnostic tool realizable.

2 AESOP experiments with Gallium

Proof-of-concept experiments for dynamic systems using Gallium vapor were begun in FY2020 and completed in FY 2021. Two different transitions in Ga were used: the $4p^2P_{1/2}$-$5s^2S_{1/2}$ ground-to-first-excited state transition at 403.4 nm and the $4p^2P_{3/2}$-$5s^2S_{1/2}$ meta-stable-to-first-excited-state at 417.3 nm. These probe beams were provided by Toptica single-mode diode laser systems with output powers up to 60 mW, mode-hop-free tuning ranges greater than 15 GHz, and linewidths less than 100 kHz without additional external stabilization. Frequency sidebands were produced in the beams at 250 Mhz by electro-optic phase modulators capable of producing modulation indices up to $\beta = 4$. The modulators were built by QuBig of Munich, Germany.

The Gallium vapors were produced by 50 mJ, 5 ns laser ablation pulses at 1.06 μm wavelength from a Q-switched YAG laser striking a Gallium-metal-filled, macor crucible in an evacuated steel vessel, which was back-filled with He gas to pressures of several Torr. The Helium background gas served to suppress plasma formation by the ablation pulse and to cool the atomic vapor. The probe beams traversed the vacuum vessel perpendicular to the direction of the ablation laser beam a few millimeters above the Gallium target surface before exiting the vessel and impinging on a fast detector ($f_{3dB} \geq 2$ GHz) manufactured by Photek. The resulting transmission signal in real time was recorded on a 6 GHz MSO 6-series oscilloscope from Tektronix Instruments.

High signal-to-noise (> 10) transmission data were acquired over periods of several tens of microseconds. All the data traces shown in this report are the average of ten copies of the trace, each one shifted by the period of the phase modulator RF drive, $\tau = \dfrac{1}{\nu_{Mod}}$, before averaging. In addition to this averaging some of the traces shown later in this document were smoothed by a moving average with an averaging window of 4 ns. This latter smoothing was only done for display purposes and is noted in the figures.

A typical time trace for the ground-state transition is shown in Fig.1. The probe beam was gated by an acousto-optic modulator (AOM), so the first part of this trace shows the quiescent system signal with no laser beams traversing the vacuum vessel. The probe laser is switched on at approximately 8 μs resulting in the roughly 5 mV signal from the unattenuated beam striking the detector. Just before 20 μs a single ablation pulse strikes the Gallium surface producing a plume of vapor that enters the probe beam causing dispersion and absorption of the probe beam, evident in the nearly 100% amplitude modulation of the signal beginning immediately after the ablation pulse. This dispersion signal persists, but with decreasing amplitude, until the AOM shuts off the probe beam at roughly 95 μs.

Short time segments of data, typically 40 ns long, at various times throughout the full time record were compared with simulations from a Mathematica code that implements a complex error function package. The code calculates the transmitted probe beam intensity, normalized to the incident intensity, resulting from the frequency-dependent dispersion and absorption in a vapor of user-specified column density, ρ and Doppler temperature, T, taking into account all the electric-dipole-allowed transitions in each of the isotopes present in naturally occurring Gallium metal and using the parameters such as probe laser detuning and modulation index from the particular experiment being modeled. This calculated trace is then convolved with the time-response function of the Photek detector as measured by
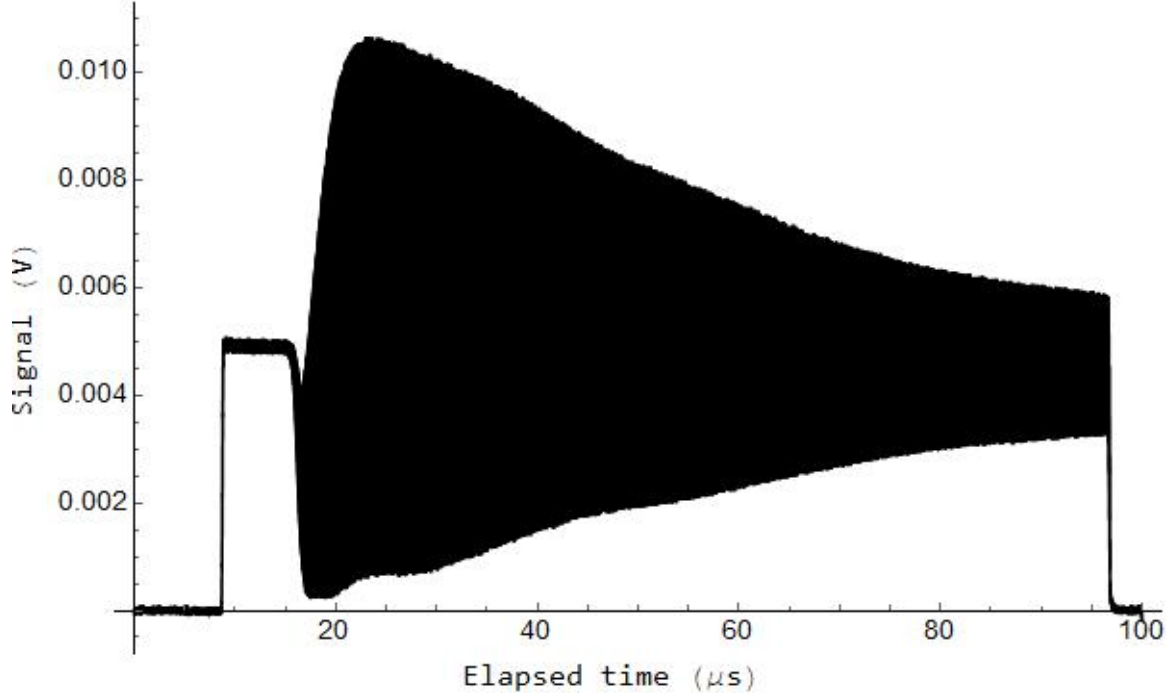
Figure 1: Raw signal returned by the AESOP diagnostic in Gallium vapor.

personnel at the Special Technologies Laboratory (STL).

Overlays of 40 ns of normalized transmission data, $\dfrac{I_{Trans}(t)}{I_{Inc}}$, and simulation results at two different times during the plume evolution are shown in Fig.2. It is important to point out that these overlays are not the result of a fitting algorithm. Rather, the Doppler temperature and column density are chosen manually to provide the best fit as judged by the user. In the future we will implement a fitting algorithm based on the minimization of the χ^2 surface in ρ-T parameter space. That change will place the analysis on a more quantitative footing and enable determination of the uncertainty in the fit parameters. Presently, we note that a 10% change in either of the simulation parameters results in easily discernible changes in the simulation, giving an indication of the level of certainty to which the parameters can be determined.

If we do this exercise at multiple times, we can map out the time evolution of the Doppler temperature and column density of the vapor plume. Figure 3 shows the results over an interval covering 70 μs. In this figure, the data from Fig.1 have been normalized so that the initial probe beam intensity is equal to one and smoothed with a 4 ns moving average for ease of viewing. Immediately after the ablation pulse, the vapor cools quickly, dropping over 200 K in less than 5 μs but thereafter cools only by another 75 K in 55 μs. The ground-state column density drops by roughly 10% in the first 5 μs or so before falling by almost a factor of 5 in the next 65 μs.

The work described in Section 2 fulfills the completion criteria of the FY2021 Campaign 3 AESOP Work Package Phase 1 L3 Milestone: Finish AESOP proof-of-concept experiments using an atomic Gallium dynamic vapor laser ablation source, analyze the results and compare with simulations.
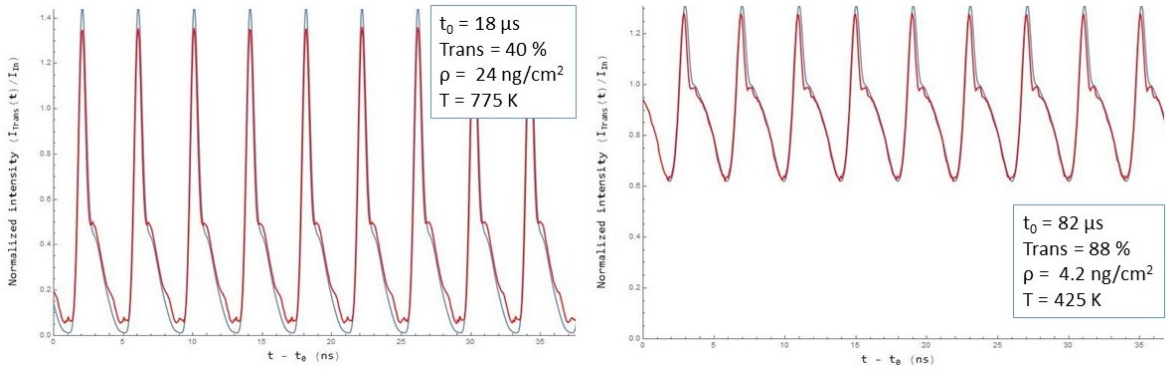
Figure 2: Normalized transmitted laser intensity data (red) and simulations (blue) at two different times, t_0, with the column density, ρ, and Doppler temperature, T, used in the simulation shown in the legends.
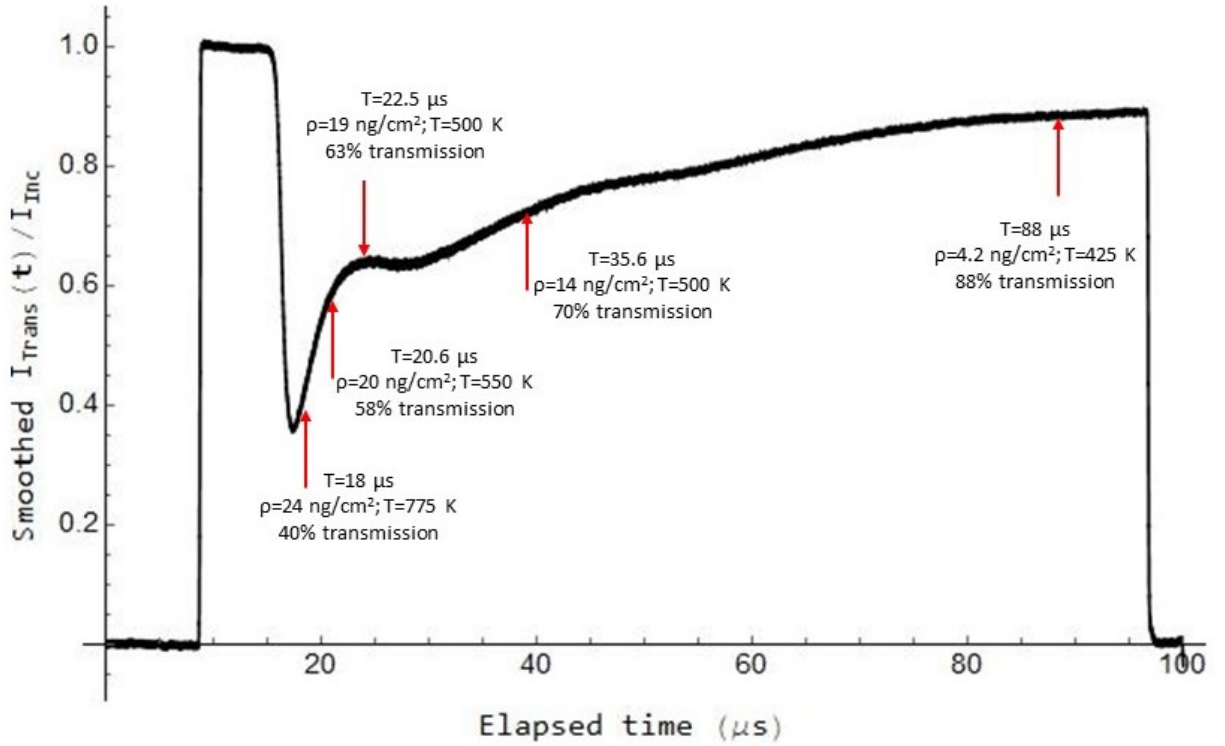

Figure 3: Normalized transmitted laser intensity as a function of time, after additional smoothing with 4 ns moving average window, with the results of model simulation at various times overlaid on the trace showing the evolution in time of the column density and Doppler temperature of the Gallium vapor plume.
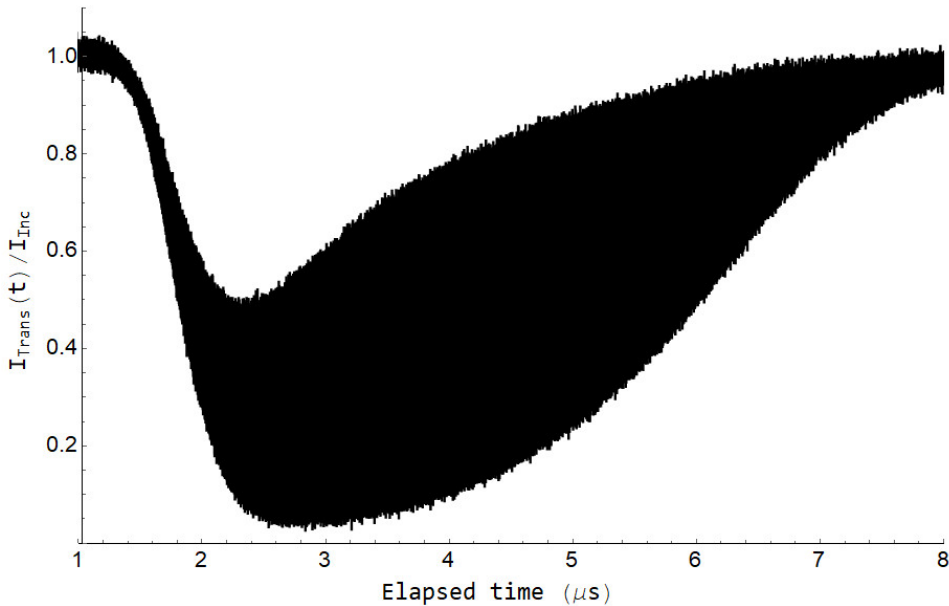
Figure 4: Normalized transmitted laser intensity returned by the AESOP diagnostic in laser-ablation-produced Cerium vapor.

3 AESOP experiments with Cerium

We chose Gallium for our initial feasibility studies due to the accessibility of the electronic transition wavelengths to diode laser technology and the relative ease of working with Gallium metal. However, the next phase of this work requires gas gun experiments, and Gallium is unsuitable for such a platform due to its tendency to form alloys with any surrounding metals. Instead, we used Cerium for the next phase of the diagnostic development, first in the same laser ablation system and then on the gas gun facility at STL.

The 593 nm wavelength light used to drive the transition from the $4f5d6s^2$ ($^1G_4$) ground state to a high-lying excited state at $E = 16869.25$ cm^{-1} was again provided by a Toptica laser system, although this wavelength required second-harmonic generation of a amplified diode laser. This exquisitely engineered system provides up 200 mW of 592.8 nm laser light with a similar mode-hop-free tuning range and linewidth as the diode-only system used in Gallium in a robust, turn-key system. The beam was phase-modulated using the same electro-optic phase modulator as in the Gallium system.

3.1 Laser ablation studies

Figure 4 shows the normalized transmitted laser intensity as a function of time starting after the AOM has switched on the 592.8 nm laser beam but before the ablation pulse has arrived at the Cerium metal target surface. The same amplitude modulation is evident in this trace as in the Gallium vapor trace of Fig.1, albeit with smaller amplitude and a shorter duration. The analysis of the data is done in exactly the same way as that of the Gallium data with the obvious difference that the atomic physics parameters used are those for Cerium.

Figure 5 shows representative results at 2.9 μs and 6.6 μs in the signal trace, corresponding
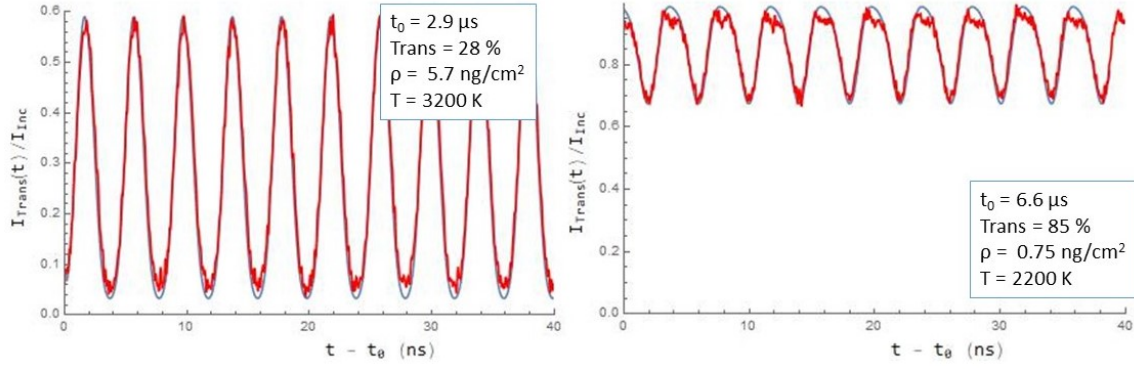
5

Figure 5: Normalized transmitted laser intensity data (red) and simulations (blue) for Cerium vapor at two different times, t_0, with the column density, ρ, and Doppler temperature, T, used in the simulation shown in the legends.
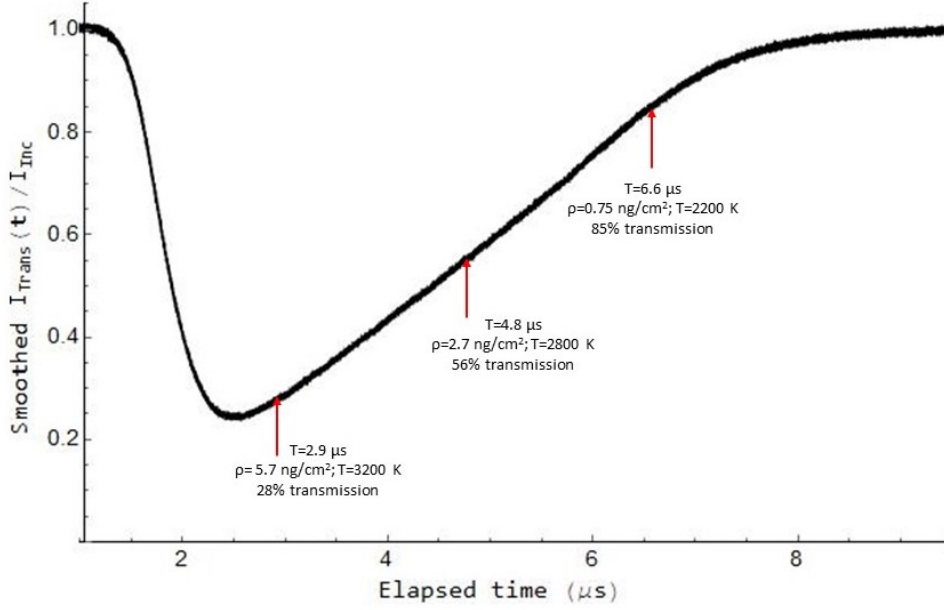

Figure 6: Normalized transmitted laser intensity as a function of time, after additional smoothing with 4 ns moving average window, showing the time evolution of the Cerium vapor parameters.

to 28% and 85% normalized transmission levels, respectively. In general, lower column densities with higher temperatures result, which is perhaps not surprising given the higher melting temperature of Cerium metal relative to Gallium. The same *caveat* applies to these results as for the Gallium simulations: these are not quantitative fits but result from manual selection of fitting parameters. Figure 6 shows the time evolution of the column density and temperature of the Ce vapor.

The work described in Section 3.1 fulfills the completion criteria of the FY2021 Campaign 3 AESOP Work Package Phase 2 L3 Milestone: Perform AESOP diagnostic development studies using an atomic Cerium dynamic vapor laser ablation source, analyze the results, and compare with simulations.
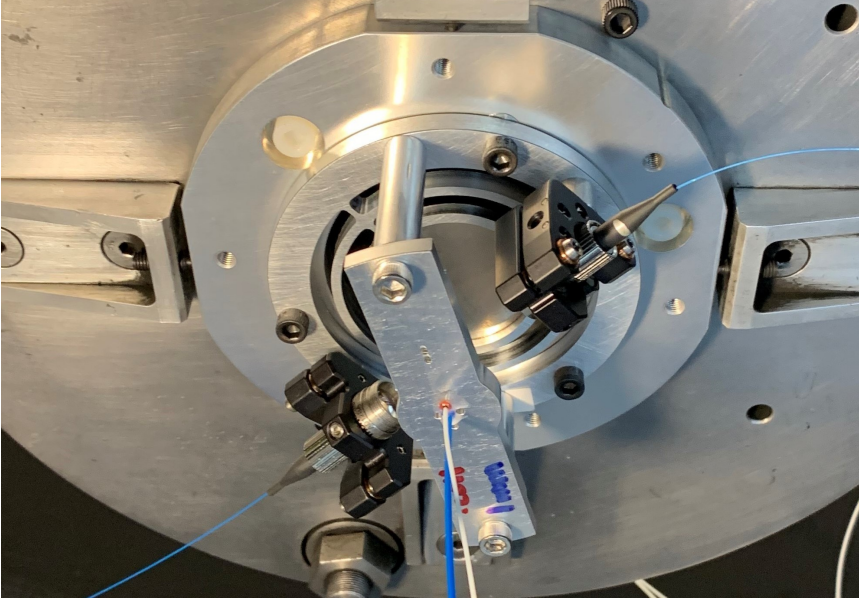
Figure 7: The experimental package mounted on the gas gun showing the AESOP probe beam input and collection fibers (thin blue cables), the Doppler velocimetry fiber (white), and the radiance collection fiber (thick blue). The white leads behind the mounting plate are trigger signal cables.

3.2 Gas gun experiments

Vapors produced by shocked metal surfaces, such as in a gas gun, are of more interest than those produced by laser ablation heating of the surface. However, shocked surfaces can also produce macroscopic ejecta, which can obscure effects arising from the atomic vapor and certainly complicate the analysis of any vapor data. Mie or Rayleigh scattering of light from the probe beam mimics absorption by the vapor and produces a position-dependent probe beam intensity in the vapor. In the worst case, the macroscopic ejecta field could be so dense that no probe beam light reaches the detector.

Macroscopic ejecta are known to be produced by surface roughness through Richmeyer-Meshkov instability of the expanding liquified target surface or through multiple shock interactions within the target. Our initial experiment was therefore a single-shock experiment in a 40 mm diameter Cerium target with surface roughness $R_a \leq 100$ nm shocked by a Tungsten impactor travelling at 2.3 km/s in the STL gas gun thereby producing a peak stress of about 50.3 GPa in the target. Despite the single-shock design and the relative smoothness of the target surface, Doppler velocimetry measurements of the expanding target free surface clearly showed significant amounts of ejecta traveling ahead of the free surface.

The collimated AESOP diagnostic probe beam traversed the Cerium vapor cloud 27.5 mm downstream from the pre-impact target surface and was collected by a multimode fiber/fiber optic collimator and coupled to a high-speed photodiode from Hamamatsu. From the 35 mm diameter of the impactor we estimate the probe beam path length through the Cerium vapor to be roughly 30 mm. Figure 7 shows a close-up of the target and probe beam arrangement once it was mounted on the gas gun.

Figure 8 shows the normalized, transmitted-probe-laser intensity as a function of time. The signal shows a smooth transition from full intensity to complete extinction of the beam in about 1 μs, which is consistent with the presence of macroscopic ejecta particles scattering light out of the collection optics acceptance angle with the gradual extinction
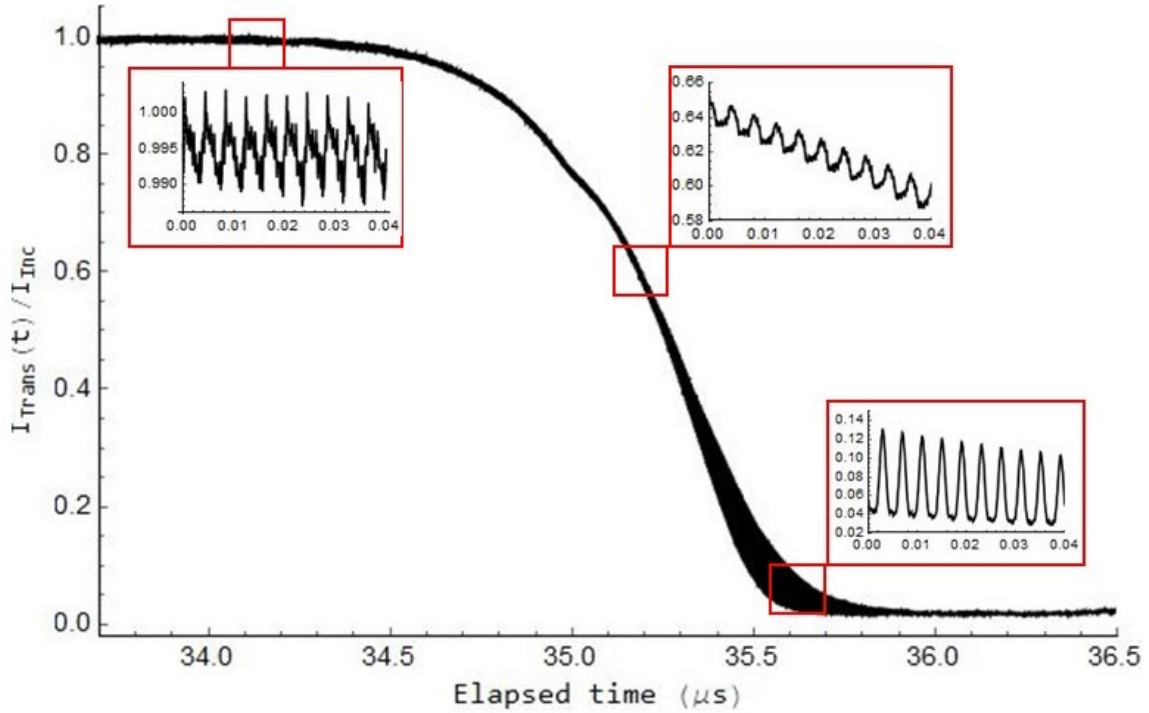
Figure 8: Normalized transmitted laser intensity from first AESOP Ce gas gun experiment showing ejecta obscuration of the probe beam with AESOP signal modulating the extinction curve as shown in the insets. Placement and size of the inset boxes is not to scale.

due to increasing particle density or size and the finite diameter of the probe beam, ~ 2 mm in this case.

Forty-nanosecond-duration windows starting at 34.0 μs, 35.15 μs, and 35.55 μs are shown in three insets in this figure. The earliest time window shows a periodic signal at the phase modulator frequency on the undiminished probe beam. We believe this signal to be due to residual amplitude modulation, not the presence of any Cerium vapor. Although the origin of this signal is not clear in this case, residual amplitude modulation in the output of electro-optic phase modulators is always present, albeit usually at insignificant levels. Note that the amplitude of the signal corresponds to $\sim 0.5\%$ of the incident beam intensity and can likely be reduced by improved system alignment..

At the later times, larger amplitude signals at the relevant frequency are clearly evident on the probe beam despite the diminishing beam intensity. This behavior is consistent with a mixture of macroscopic ejecta particles and Cerium vapor of varying densities moving across the probe beam with the non-zero lower bound of the AESOP modulation signal resulting from the unobstructed part of the beam striking the detector.

The complicated time-varying composition of the cloud makes it impossible to extract an atomic Cerium ground state column density and temperature from the data. We simply note that the general form of the modulation, sharp peaks with broader, flatter valleys, is consistent with an atomic Cerium ground state column density of a few ng/cm^2 and Doppler temperatures ~ 2200 K for the laser detuning and modulation index of this experiment.

The Doppler temperature was chosen since the radiance measurements yield a surface temperature of 2200 K.

The work described in Section 3.2 fulfills the completion criteria of the FY2021 Campaign 3 AESOP Work Package Phase 3 L3 Milestone: Setup and perform first AESOP diagnostic development experiment using a Cerium gas gun driven ejecta source, analyze results and compare with simulations.

4   Conclusion

We have demonstrated that the AESOP diagnostic will work on various elements in dynamic environments for column densities < 1 ng/cm^2. Higher column densities can be measured by increasing the probe beam detuning appropriately. We have demonstrated that the diagnostic can be fielded on gas gun experiments, but the effects of macroscopic ejecta particles must be countered. Future experiments will employ an additional non-resonant beam, detuned by tens of nanometers from the vapor transition wavelength, to correct the measured transmitted AESOP probe intensity for the scattering and absorption due to Mie/Rayleigh scattering leaving the pure AESOP signal. Implementation of this correction technique will be the focus of future work.

This document and the work discussed in it constitute completion of the FY2021 Campaign 3 AESOP Work Package L3 Milestones in total.

Acknowledgements

References

[1] J.A. Paisner and M.M Schauer, Linear Propagation of Near-Resonant, Sinusoidal-Phase-Modulated, Laser Light through an Atomic Vapor Column Density, LA-UR-20-29533, Version 1 November 2020, Version 2 June 2021